Available online at www.CivileJournal.org

Civil Engineering Journal

(E-ISSN: 2476-3055; ISSN: 2676-6957)

Vol. 12, No. 06, June, 2026

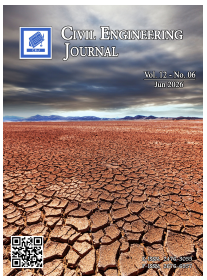

Study on the Structural Performance of Pre-Damaged Perforated Wide Shallow RC Beams Repaired with CFRP Composites

Bashar F. Abdulkareem [1*], Nameer N. Salman [2], Nooralmustafa Ali [2], Mustafa Abdulkdir [1]

[1] *Department of Reconstruction and Projects, University of Baghdad, Baghdad 17001, Iraq.*

[2] *College of Engineering, Al-Nahrain University, Baghdad 10071, Iraq.*

Received 07 March 2025; Revised 09 May 2026; Accepted 11 May 2026; Published 01 June 2026

Abstract

This research presents the results of a numerical simulation conducted using ABAQUS/CAE finite element software. The research sought to establish a simulation model capable of predicting the structural performance of pre-damaged perforated wide shallow reinforced concrete (RC) beams repaired with different Carbon Fiber Reinforced Polymer (CFRP) composites. Numerous investigations on CFRP composites in perforated wide beams are few, characterized by low representational precision and inferior material quality. The findings were assessed against published experimental data in the current literature. The numerical method and the experimental data were very similar; hence, the simulated model was considered legitimate. Subsequently, the scope of numerical studies was expanded to include the examination of several factors, including the pre-damage percentage, aperture configuration, and the number of openings. The results show that the percentage of damage is inversely proportional to the load-carrying capacity of the wide beams. Wide beams with circular openings have a higher load-carrying capacity than those with square openings. Using circular openings instead of square ones increases strength by about 11.3%, 25.4%, and 36.5% for three, five, and seven openings, respectively. Despite openings that weakened the wide beams, strengthening with CFRP laminates restored their load-bearing capacity and even exceeded it. The increase in load-bearing capacity of the strengthened perforated wide beams ranged from 82% to 161% compared to the un-strengthened solid wide beam.

Keywords: Wide Beam; Perforated Beams; Pre-Damaged; CFRP Composites; Stiffness; Absorbed Energy; ABAQUS.

1. Introduction

Shallow/wide beams are characterized as beams with a width exceeding double their depth (width/depth < 2) [1]. Many floor designs use wide beams to move floor loads to columns. In bridge construction, a design using wide, shallow beams may offer a straightforward, cost-effective approach to transferring loads from the slab deck to the columns. In many design situations, using different member widths is advantageous for alleviating reinforcing conflicts and reducing overall congestion. The standard approach involves using beams that exceed the width of the supporting columns. The geometric disparities in element width between the beam and the column will result in a unique force distribution in the beam, unlike in beams that support columns of identical breadth. Wide beams are a favored, cost-effective choice for projects that require reducing overall structural depth. Wide beams are closely linked to time efficiency, as they facilitate the construction of formwork and reinforcement. Wide beams effectively manage cracking and deflection requirements while alleviating congestion in the reinforcement. Using wide beams made of reinforced concrete offers several benefits. Reduce floor height in construction projects such as warehouses, commercial buildings, parking garages, and office

* Corresponding author: b.faisal1101@coeng.uobaghdad.edu.iq

https://doi.org/10.28991/CEJ-2026-012-06-012

buildings to facilitate the operation of services below the floor. For beams characterized by substantial width and little depth, the terms "wide beam," "shallow beam," and "banded beam" are mostly synonymous [2, 3].

The use of perforations in broad beams makes them lighter and easier to carry, and improves their geometric adaptability. Nonetheless, inclusion apertures would complicate the beam's behavior, as they cause a sudden change in its cross-sectional dimensions. However, the corners of the holes may experience higher stress concentrations, potentially leading to significant cracking, which is undesirable from both aesthetic and durability standpoints. The decreased rigidity of the beam may lead to excessive deflection under service loads and cause significant redistribution of internal stresses in a continuous beam [4-6]. The reduction in rigidity caused by the holes may be mitigated by reinforcing the FRP composites. The use of Fiber Reinforced Polymer (FRP) composites as a reinforcement material in the construction industry has been in use for about 30 years. The worldwide prevalence of strengthening applications using Fiber Reinforced Polymer (FRP) is increasing, driven by the growing acceptance of this method and the establishment of comprehensive design standards. The use of CFRP composites has focused on flexural reinforcement, in which CFRP sheets or laminates are affixed to the upper or lower surfaces of beams at points experiencing the greatest bending moments [7-9].

A study by Lotfy et al. [10] examined the impact of shear reinforcement on shear strength, shear cracking, ductility, and failure modes of shallow concrete wide beams. The primary factors examined in this study were: shear reinforcement ratio, shear span-to-depth ratio (a/d), stirrup spacing and quantity of vertical branches, and stirrup spacing-to-depth ratio (s/d). The specimens were categorized into two groups, each including five beams: one reference beam without shear reinforcement and four beams featuring varying shear reinforcement configurations. Test findings indicate that shear reinforcement significantly influences shear strength, failure mode, and ductility of shallow wide beams.

Conforti et al. [11] presented the findings of Polypropylene Fiber Reinforced Concrete Wide-Shallow Beams (PFWSBs) subjected to shear, emphasizing the significance of the width-to-effective depth ratio (b/d) and the advantageous effects of newly developed fibers. Results indicate that the capacity of polypropylene (PP) fibers to exhibit significantly stable shear behavior was empirically shown, along with the potential use of PP fibers as minimal shear reinforcement.

El-Sayed et al. [12] examined the long-term deflection and cracking properties of WSBs reinforced with CFRP laminates. Five full-scale WSBs were fabricated: two beams underwent static loading tests, while three beams were subjected to sustained loading for a duration of 601 days. Three samples were reinforced with CFRP laminates adhered to their soffits, while two beams remained unreinforced, functioning as controls. Beams reinforced with CFRP plates exhibited considerable enhancement in short-term deflections and fracture width relative to the unreinforced beam. The reinforced beams, nevertheless, exhibited minimal enhancement in long-term performance. The efficient modulus method was found to accurately forecast the supplementary long-term displacement of the beams using the concrete creep model.

Chin et al. [13] investigated the behaviour of reinforced concrete (RC) beams with significant apertures strengthened with externally bonded CFRP laminates. Six simply supported beams, consisting of two solid specimens and four with apertures, were constructed and subjected to four-point bending tests. Each beam had a cross-section of 12 × 30 cm and a length of 2 m. Each beam had a significant opening symmetrically located at its center. The test parameters included the configuration and measurements of the opening, as well as the reinforcing layout for the CFRP laminates. The investigation was conducted via experimental testing and finite element analysis. The experimental results demonstrate that the inclusion of a significant mid-span aperture reduces the beam's capacity by nearly 50%. The testing results demonstrated an 80–90% increase in strength due to CFRP laminate reinforcement. The numerical results were juxtaposed with the experimental findings.

Abass & Hassan [14] presented the test outcomes of four full-scale WSBs. One beam was unstrengthened, while the other three were reinforced with CFRP sheets adhered with epoxy, varying in width within the flexural zone: one beam was strengthened with 30% of the cross-section width, another with 60%, and the third with 100%. All beams have identical sizes and reinforcement ratios. The test findings indicated that the beam reinforced with (60%b) exhibited the superior flexural capacity relative to the other reinforced beams. This beam enhances flexural capacity by up to 29% compared to the control beam.

Al-Abdwais & Al-Mahaidi [15] documented an experimental study of the behavior of small-scale retrofitting beams using a Near-Surface-Mounted strengthening method with CFRP textiles, laminates, and cement-based adhesives for flexural applications. The beams repaired with modified cement-based adhesive attained ultimate loads ranging from 98% to 100% of those strengthened with epoxy adhesives. Numerical studies are employed to assess the experimental outcomes, revealing equivalent findings between the experimental results and finite element analysis.

Al-Kamaki [16] employed a hybrid methodology to improve the properties of the reinforcing beams by integrating high-strength CFRP with FRP composites using epoxy glue. Five reinforced concrete beams measuring 23 × 26 × 160 cm were subjected to pre-loading at 75% of the maximum load of the control beam, subsequently pre-damaged,

strengthened, and evaluated under a three-point bending configuration. One beam functioned as an unreinforced control, while another was reinforced with a single layer of CFRP at the beam's centerline. The remaining three beams were reinforced with a CFRP plate, incorporating supplementary anchorage at the ends utilizing CFRP, BFRP, or GFRP sheets. The reinforced beams demonstrated a substantial enhancement in ultimate load compared to the reference beam. The application of CFRP strengthening with U-wrap increased the ultimate load of RC beams by up to 45% compared with the unstrengthened beam. In contrast, deflection decreased by roughly 64%, indicating enhanced strength and stiffness.

Badawy et al. [17] examined the flexural performance of high-strength concrete WSBs utilizing hybrid longitudinal reinforcement comprising steel and ribbed glass fiber-reinforced polymer (GFRP), as well as ribbed basalt fiber-reinforced polymer (BFRP). A cohort of six half-scale WSBs was analyzed, possessing dimensions of 2.1 m in length (L), 0.6 m in width (B), and 0.25 m in depth (d), maintaining a constant size effect (d/B). The initial three examples were entirely strengthened on the stress side with steel, GFRP, or BFRP ribbed bars, serving as control specimens. The incorporation of GFRP and BFRP bars increased the flexural capacity of SWB by 41% and 43%, respectively, in comparison to specimens reinforced with steel only.

Palaniappan et al. [18] investigated the enhancement of the strength of reinforced concrete (RC) beams by the use of CFRP laminates and CFRP composites in the flexural and shear zones of deficient RC beams. The study design included five distinct methods for enhancing pre-damaged reinforced concrete beams to their ultimate load capacity, reaching 90% of the maximum load of the reference beam. The findings indicated an important increase in the load-capacity of reinforced concrete beams externally reinforced with CFRP laminates. The beams treated with U-shaped wrapping presented a significant enhancement in both crack and failure loads. This research shows that incorporating CFRP laminates and textiles into the shear and flexural regions of pre-damaged beams can increase the final load-bearing capacity by up to 13%.

Askar [19] investigated the restoration of a pre-damaged reinforced concrete beam using recycled plastic waste and CFRP sheets. Three mixtures were formulated using two distinct lengths of Polypropylene (PP) fibers, specifically 30 mm and 50 mm, maintaining a constant ratio of 1% as advised by the literature. A total of ten reinforced concrete beams measuring (100×160×1600) mm were cast, with two serving as controls and the remaining pre-loaded to 70% of the ultimate load determined from the control specimens. The findings indicated that retrofitting pre-damaged reinforced concrete beams with CFRP composites led to a 70% increase in ultimate load when U-shaped CFRP anchoring was employed at both ends.

2. Research Significance

Few studies have been conducted on the flexural strengthening of pre-damaged perforated wide shallow RC beams using FRP composites. The goal of the project was to develop a simulation model that can predict the structural performance of pre-damaged perforated wide shallow RC beams repaired with different FRP composites, and to represent pre-existing damage in the finite element model accurately. Figure 1 illustrates the research approach flowchart.

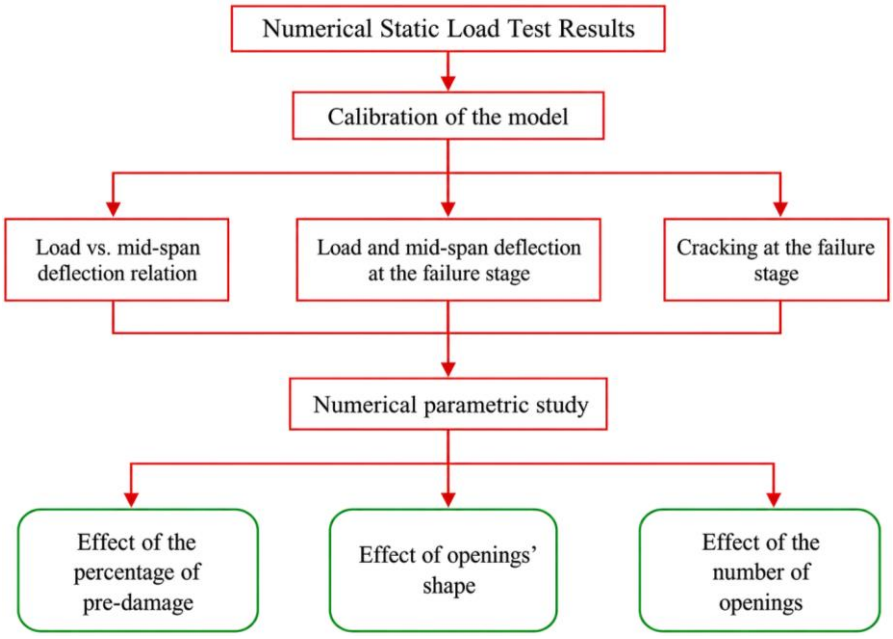

Figure 1. Flowchart for the research methodology

3. Test Specimens

The experimental program by Al-Negheimish et al. [20] and Al-Zaid et al. [21] included testing four wide, shallow RC beams (with and without pre-damage) subjected to monotonic loads. All wide beams have a cross-section dimension of 500 x 250 mm and an overall length of 5300 mm. The primary bottom rebars were four 16 mm in diameter, while the primary top bars were four 12 mm in diameter. Figure 2 illustrates the specifics of the assessed beams. Table 1 presents the results of the mix of concrete qualities. Table 2 presents the parameters of the steel rebars. The CFRP laminates possess a low modulus of elasticity (L) of 165 GPa, f_u = 2800 MPa, ε_f =16970 µmm/mm, and have a thickness of 1.4 mm. Table 3 shows the details of the tested wide beams.

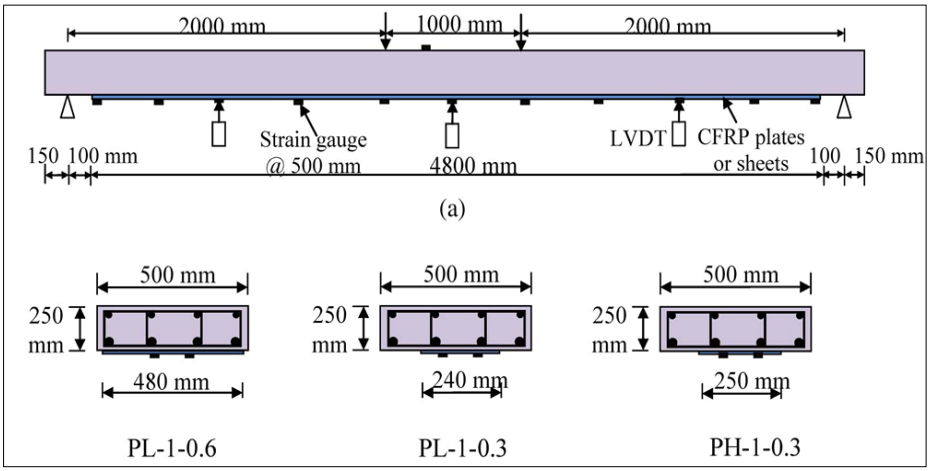

Figure 2. Details of adopted wide beams [20, 21]

Table 1. Data of concrete mix [20, 21]

Compressive strengths (MPa)	Splitting tension strength f_{ct} (MPa)
30	3.07

Table 2. Test of steel bars [20, 21]

Bar diameter (mm)	Area of cross-section (mm²)	*fy* (MPa)	*fu* (MPa)	E_S (GPa)
8	50.3	387	490	200
12	113	533	700	207
16	201	562	700	205

Table 3. Details of the tested wide beams [20, 21]

Beam ID	CFRP width (mm)	Pre-loading percentage (%)*	Reference No.
PL-1-0.6	480	0	Al-Negheimish et al. [20]
PL-1-0.3	240	0	
B-0.6-0.3	480	35	Al-Zaid et al. [21]
B-0.3-0.5	240	55	

* Pre-loading percentage from the ultimate load of the control beam = 98.4 kN.

4. Modeling and Analysis of Examined Wide Beams

This investigation uses the Finite Element Technique to examine wide beams with the ABAQUS CAE 2022 program, specifically the Standard/Explicit Model [22]. The isoperimetric eight-node brick element (C3D8R) was used to depict the concrete broad beams, load plates, and support plates. For the reinforced steel rebars, the truss element (T3D2), a 3-D two-node bar member that exhibits movement in the x, y, and z axes, was used. A Shell section with the necessary thickness (S4R: A 4-node doubly curved shell, employing decreased integration, hourglass control, and adapting finite membrane strains). Fabricating components entails designing discrete elements by the delineation of their geometrical configurations, such as a rectangular concrete beam, steel reinforcement, and a CFRP laminate. To complete all specimens in the ABAQUS environment, many parts were produced as shown in Figure 3. The supports at the extremities of the wide beam were represented as simply supporting. Figure 4 delineates the restrictions of boundary and load parameters.

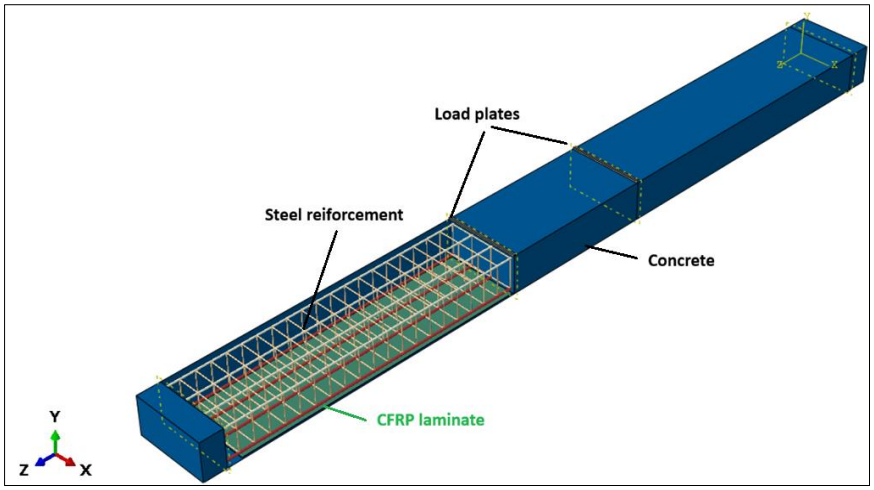

Figure 3. Creating parts and assemblies in ABAQUS

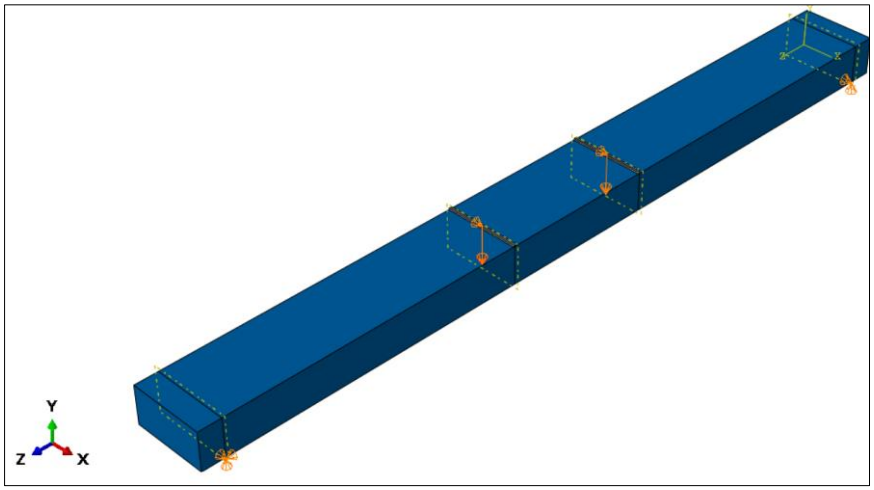

Figure 4. Parameters of boundaries and loads

For a comprehensive assessment of the interaction, the steel reinforcement is assumed to be entirely encased in concrete. A Tie-type interaction restriction was established between the concrete component and the plates of the supports and loads. A Tie-type interaction limitation was established between the concrete component and the CFRP laminates, as seen in Figure 5. Table 4 illustrates the input information for concrete damage plasticity. Tables 5 and 6 display the compressive and tensile findings for concrete, respectively, computed according to Majumder & Saha [23] based on the values of fc' and f_{ct} from Al-Negheimish et al. [20]. The characteristics of steel reinforcement and CFRP laminate are delineated in Tables 2 and 3, respectively.

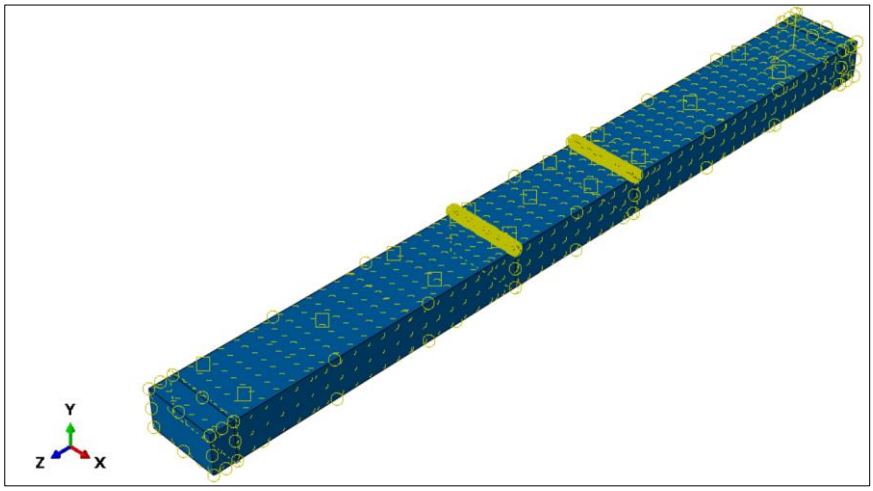

Figure 5. Interaction of the components

Table 4. Inputs details for damage plasticity of concrete

Elasticity modulus (MPa)	Poisson' ratio	Dilation angle (degree)	Eccentricity	$\epsilon_{bo}/\epsilon_{co}$	Viscosity
25742	0.17	40	1.16	0.667	0

Table 5. Concrete compressive information

Yield-Stress (MPa)	In-elastic Strain
11.62421459	0
17.2272561	0.00005
22.03847026	0.000229564
25.7165319	0.00044479
28.19158637	0.000742978
29.58461774	0.001129769
30	0.001585803
28.84318275	0.002611683
26.22895917	0.00376223
23.20452528	0.004937353
20.31178576	0.006091356
17.67413538	0.007243632
15.41104568	0.008362563
8.392454915	0.013583081
5.117675848	0.018612782
3.431677365	0.023496721
2.464355313	0.028270615
1.844737835	0.033104346
1.434007368	0.037894161

Table 6. Concrete tensile information

Yield-Stress (MPa)	Strain
3.070	0.0
1.851838281	0.000276437
1.366252052	0.000501676
0.801191519	0.001112684
0.583345815	0.001698494
0.411738988	0.002660946
0.323273866	0.003617366
0.268545513	0.004571339
0.231031382	0.005524062
0.203559149	0.006476055
0.182487739	0.007427585
0.094489377	0.01693397
0.066177544	0.026436024
0.051767861	0.035937071
0.0429115	0.045437713
0.036865024	0.054938152
0.032449036	0.064438473
0.029068541	0.073938719

To account for the deteriorated response of concrete, two distinct uniaxial compressive and tensile damage variables, dc and dt, are defined in the concrete damage plasticity (CDP) model. These variables denote the damage to elastic stiffness that happens when a concrete specimen is unloaded from any point on the strain weakening segment of the stress-strain graphs. The deterioration in elastic stiffness differs markedly between compressive and tensile characteristics. The uniaxial deterioration variables depend on plastic stresses, temperature, and field variables. The values range from 0 to 1, representing intact and fully damaged materials, respectively [24]. The compressive and tensile damage behaviors of the concrete, as defined in the finite element material model, are illustrated in Figure 6.

$$d_c = 1 - \frac{\sigma_c E_c^{-1}}{\varepsilon_c^{pl}\left(\frac{1}{b_c}-1\right)+\sigma_c E_c^{-1}} \quad (1)$$

$$d_t = 1 - \frac{\sigma_t E_c^{-1}}{\varepsilon_t^{pl}\left(\frac{1}{b_t}-1\right)+\sigma_t E_c^{-1}} \quad (2)$$

where, $\varepsilon_c{}^{pl}$ and $\varepsilon_t{}^{pl}$ are plastic strains for compression and tension respectively.

$$\varepsilon_c^{pl} = b_c\,\varepsilon_c^{in}, \quad b_c = 0.7 \;\; and \;\; \varepsilon_t^{pl} = b_c\,\varepsilon_t^{in}, \quad b_t = 0.85$$

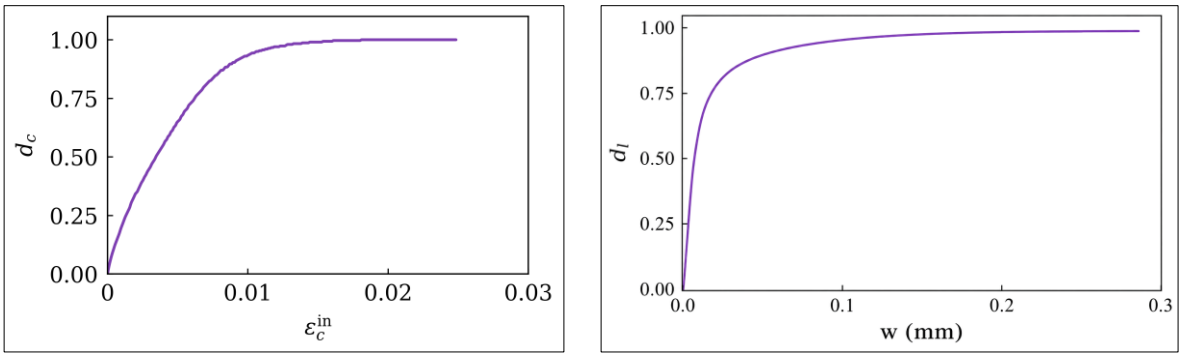

(a) Compression damage (b) Tension damage

Figure 6. Damage behaviors of the concrete [24]

5. Definition of Pre-loading (Pre-damage) in ABAQUS

Here, the control (un-strengthened) wide beam is used by copying it and modifying the load from a load-up-to-failure to one limited by the pre-load percentage, for example, 30% of the ultimate load (p1) of the control model. This load is then applied gradually using the amplitude command, as shown in Figure 7-a. After that, in the step module, intervals must be created to output results that can be recalled later in the strengthened model, as shown in Figure 7-b. Finally, the job is given a unique name for later retrieval of results, for example, Job 22.

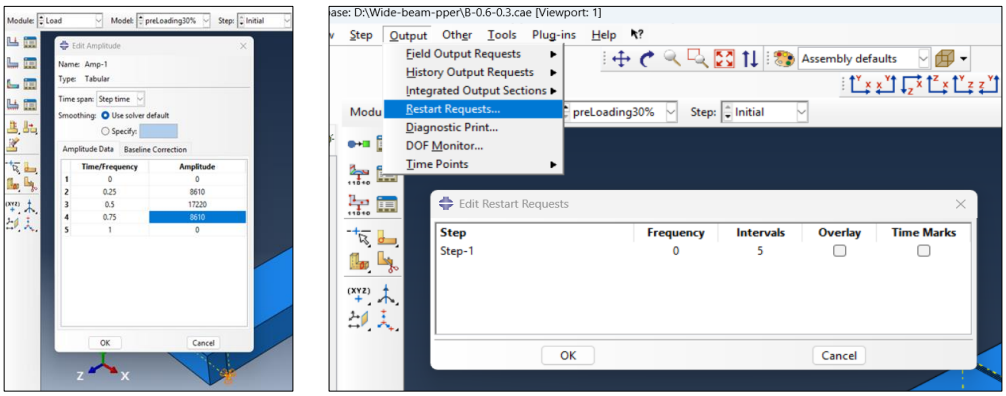

(a) Amplitude of pre-load (b) Intervals of output results

Figure 7. Amplitude of pre-load and intervals of output results

The next step is to duplicate the previous model and name it after the last stage (post-strength). Here, all required procedures are finished and the strengthening components—such as CFRP plates—are attached. Next, a load-up-to-failure is applied instead of the pre-load (P1). The first stage involves creating a designated field and retrieving the

results from the preceding model using its load module. As shown in Figure 8, every component of the model is chosen, except for the strengthening elements added in the previous model, and the necessary work (work 22) is specified. Even though the model has not yet been loaded (increment zero), Figure 9 demonstrates that the wide beam shows distortion and plastic stresses, which is a clear sign that the findings were correctly retrieved, and also shows a crack pattern match between the experimental and the numerical results.

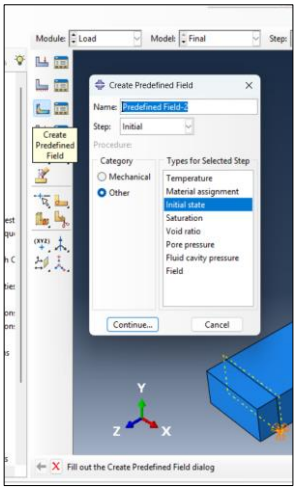

(a) Definition of predefined field

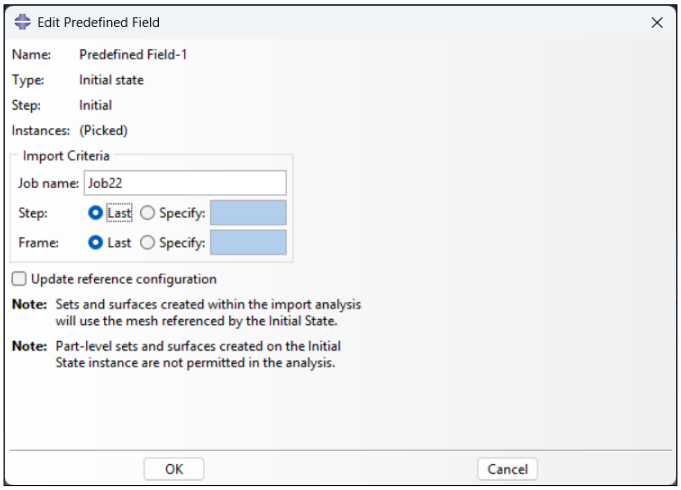

(b) Setting the job file to retrieve results

Figure 8. Definition of a predefined field

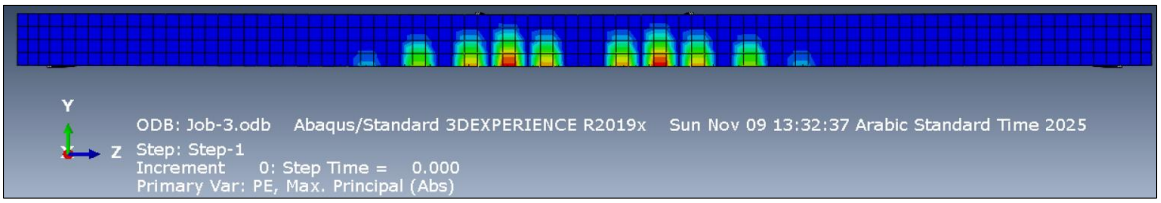

(a) Crack pattern of pre-damaged beam from Abaqus

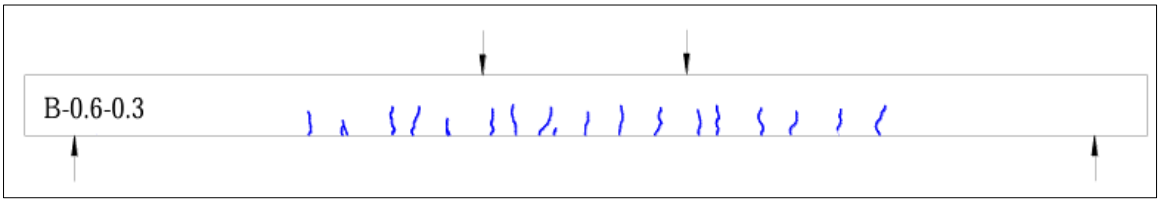

(b) Crack pattern of pre-damaged beam from experimental test of reference [21]

Figure 9. Definition of a predefined field

6. The Validation of the Fabricated Model

This part presents multiple comparisons between the experimental findings and pertinent numerical results. The areas of focus encompass the correlation between load and deflection at mid-span under static loads, as well as the evaluation of load and deflection at mid-span at the failure level. The experimental results were taken from Al-Negheimish et al. [20] and Al-Zaid et al. [21], as shown in Table 3.

6.1. Load vs. Deflection at Mid-span Curves

Figure 10 illustrates the comparison of load vs. deflection relationships at mid-span between the computational and experimental results for the wide beams. The FE models exhibited greater stiffness than the experimental results in both nonlinear and linear behaviors; yet, a satisfactory level of agreement was noted between the two. Certain factors may augment the stiffness in FEM analysis. Various factors may contribute to heightened stiffness in numerical analysis results. Microcracks resulting from curing and drying shrinkage were observed in the concrete through the experiments. These would diminish the intrinsic rigidity of the wide beam. The representation of these microcracks is lacking in numerical methods, and the connection between rebars and concrete in the finite element studies is assumed to be impeccable [25].

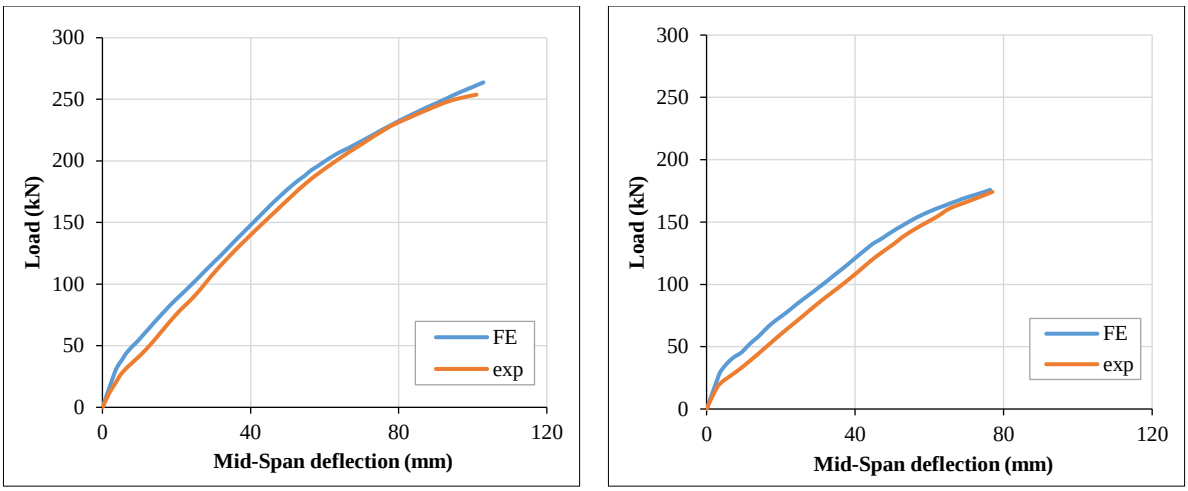

(a) PL-1-0.6 (b) PL-1-0.3

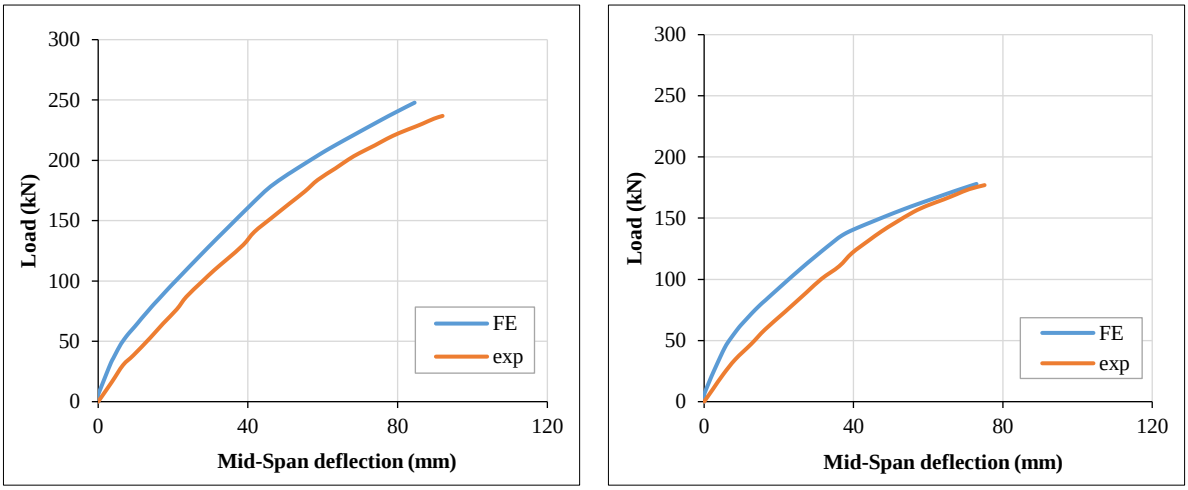

(a) B-0.6-0.3 (b) B-0.3-0.5

Figure 10. Analyzing the load against the wide beams' mid-span deflection both numerically and experimentally

6.2. Load and Deflection at Mid-Span at the Failure Level

For each sample, Table 7 compares the numerical model's predicted ultimate load and mid-span deflection to experimental data obtained at the failure level. A strong correlation was observed between the ultimate load and mid-span deflection values obtained from finite element models and from experiments, with the mean and coefficient of variation of (Pu) FE/(Pu) Ex being 1.025 and 2.0158%, respectively, for failure loads. In contrast, for deflection at mid-span (Δu_{FE} / Δu_{Ex}), they were 0.9735 and 4.269%, respectively

Table 7. Ultimate load and midspan deflection from experimental and numerical analyses

Beam ID	Failure Load (Pu)			Deflection at failure load (Δu)		
	EX (kN)	FE. (kN)	FE /EX	EX (mm)	FE. (mm)	FE /EX
PL-1-0.6	253.8	263.7	1.039007	101	102.8	1.017822
PL-1-0.3	174.2	175.8	1.009185	77	76	0.987013
B-0.6-0.3	236.8	247.8	1.046453	92	84.5	0.918478
B-0.3-0.5	177	178	1.00565	75.1	72.9	0.970706
Average			1.025	Average		0.9735
Standard deviation			0.02066	standard deviation		0.04156
Coefficient of variation (%)			2.0158	Coefficient of variation (%)		4.269

7. Numerical Parametric Study

Following the prior validation of the finite element (FE) assessment against the experimental data acquired in this study, an extensive parametric analysis was conducted using the FE model with 17 broad beam configurations, as presented in Table 8. The investigation parameters are:

- Percentage of pre- damage (undamaged, 30%, 60%, and 75%). The four damage percentages were applied to three groups (solid beams, beams with five circular openings, and beams with five square circular openings).
- Shape of the openings (circular or square);
- Number of openings (0, 3, 5 or 7).

Recognizing that all examples possess same historical characteristics of steel reinforcing and concrete

Table 8. Information on the case study of wide beams

Set	Beam name	Percentage of pre-damage (%)	CFRP laminate	Number of openings	Shape of openings
Solid	B-solid	Undamaged	Without	-	-
	B-solid-C	Undamaged	With	-	-
	B-solid-C-30	30	With	-	-
	B-solid-C-60	60	With	-	-
	B-solid-C-75	75	With	-	-
Circular openings	B-3Cir-C	Undamaged	With	3	Circular
	B-5Cir-C	Undamaged	With	5	Circular
	B-7Cir-C	Undamaged	With	7	Circular
	B-5Cir -C-30	30	With	5	Circular
	B-5Cir -C-60	60	With	5	Circular
	B-5Cir-C-75	75	With	5	Circular
Square openings	B-3Squ-C	Undamaged	With	3	Square
	B-5Squ-C	Undamaged	With	5	Square
	B-7Squ-C	Undamaged	With	7	Square
	B-5Squ-C-30	30	With	5	Square
	B-5Squ-C-60	60	With	5	Square
	B-5Squ-C-75	75	With	5	Square

7.1. Effect of the Percentage of Pre-Damage

The percentages of pre-damage used here were (undamaged, 30%, 60%, and 75%); the percentage of pre-damage represents the percentage of pre-load from the ultimate load of the control beam (B-solid) = 99.6 kN. The four damage percentages were applied to three groups (solid beams, beams with five circular openings, and beams with five square circular openings). All wide beams here (Table 9) are strengthened with CFRP laminate (the symbol C indicates that), 480 mm wide, and similar to the PL-1-0.6 beam shown in Figure 1 (see Figure 11).

Table 9. Details of the parametric study: wide beams (effect of the percentage of pre-damage); all beams in this table strengthened with CFRP

Group	Beam ID	Percentage of pre-damage (%)	Number of openings	Shape of openings
Solid	B-solid-C	Undamaged	-	-
	B-solid-C-30	30	-	-
	B-solid-C-60	60	-	-
	B-solid-C-75	75	-	-
Circular openings	B-5Cir-C	Undamaged	5	Circular
	B-5Cir -C-30	30	5	Circular
	B-5Cir -C-60	60	5	Circular
	B-5Cir-C-75	75	5	Circular
Square openings	B-5Squ-C	Undamaged	5	Square
	B-5Squ-C-30	30	5	Square
	B-5Squ-C-60	60	5	Square
	B-5Squ-C-75	75	5	Square

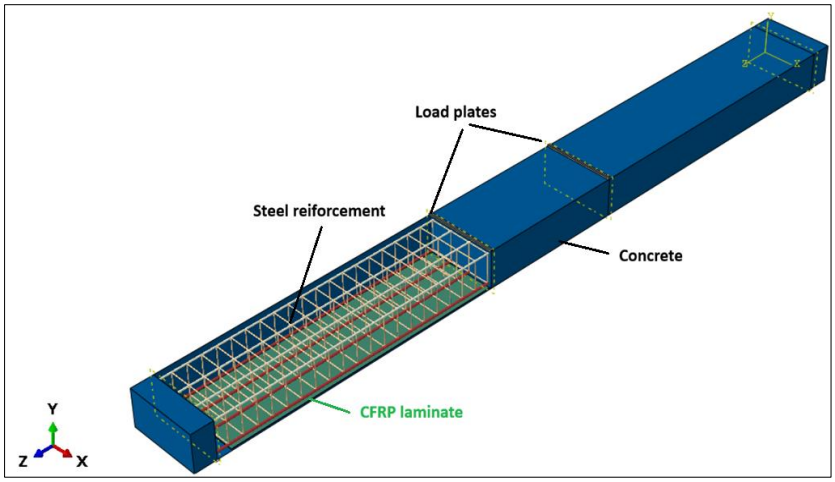

(a) Solid group

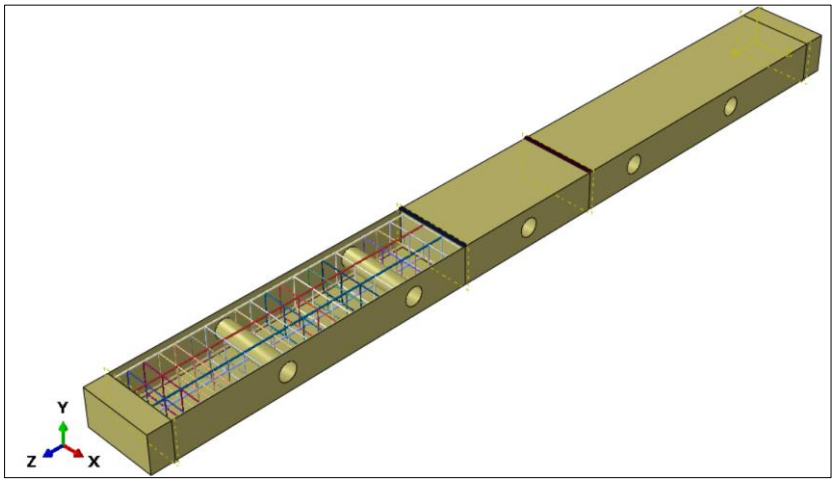

(b) Circular group

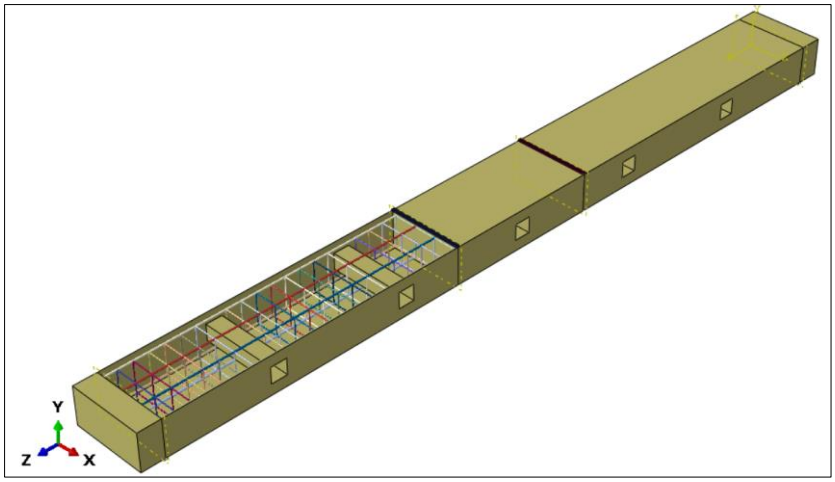

(c) Square group

Figure 11. Making components and assembling parametric study wide beams (effect of the percentage of pre-damage)

7.1.1. Load vs. Deflection at Mid-Span Relation

The influence of the percentage of pre-damage on the load vs. mid-span deflection relationship for the 3 groups is displayed in Figure 12. Based on load vs. deflection relationships, it is clear that the effect of the 30% damage percentage on reducing the stiffness of the wide beam was minimal, especially in the group of solid wide beams, likewise, the effect of the 75% damage percentage on the decrease in wide beam stiffness was significant in all groups. In general, the percentage of damage is inversely proportional to the stiffness of the wide beams, but this proportion was more pronounced in perforated wide beams than in the case of solid wide beams.

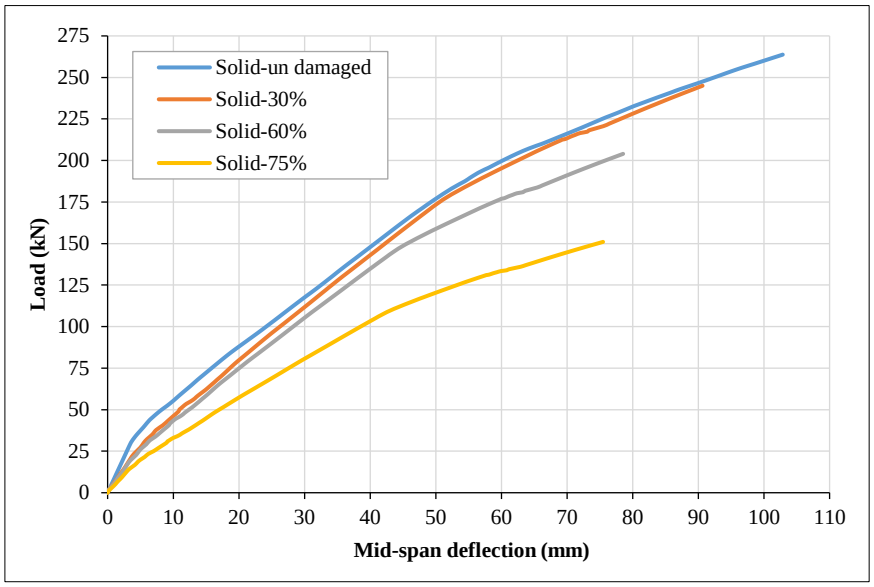

(a) Solid group

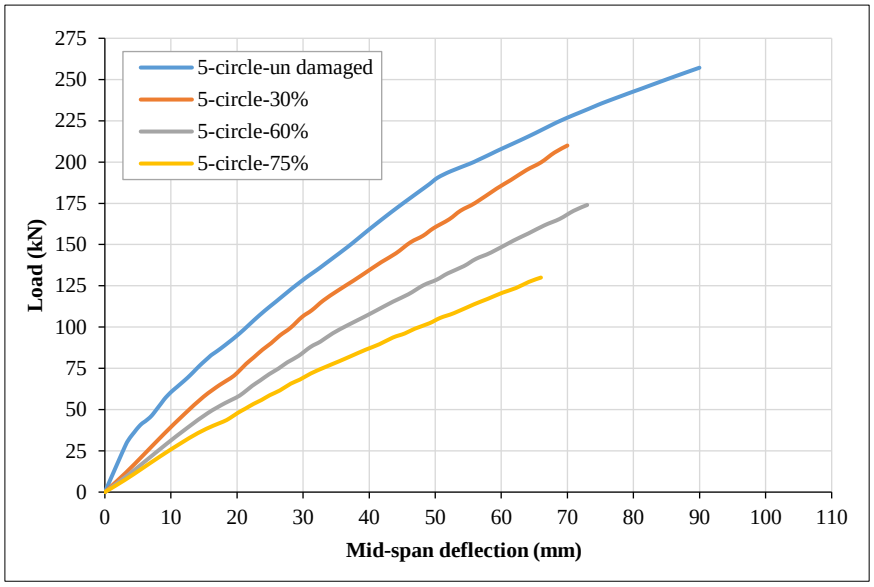

(b) Circular group

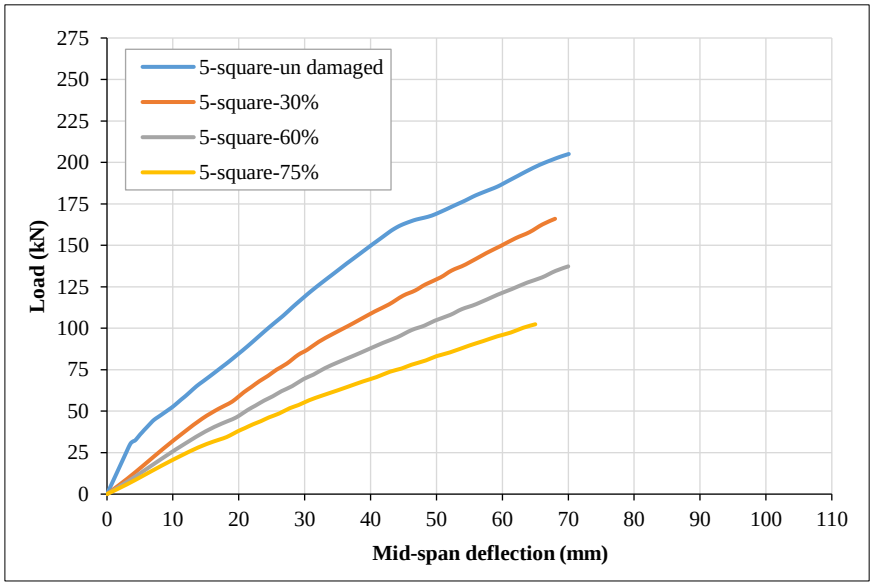

(c) Square group

Figure 12. Effect of the percentage of pre-damage on the load vs mid-span deflection relationship

7.1.2. Ultimate Load

Figure 13 and Table 10 demonstrate the influence of pre- damage percentage on the failure load. Insertion openings in a wide beam reduced the ultimate load. Using 5 circular openings instead of 5 square ones increases strength by about 25.4% and 26.7% for the undamaged and damaged wide beam, respectively.

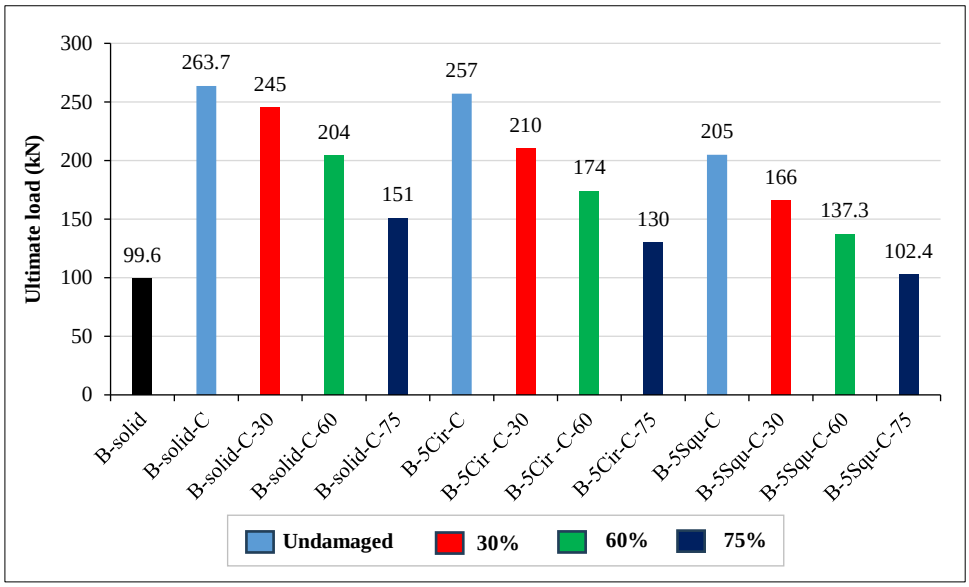

Figure 13. Impact of the percentage of pre- damage on the failure load

Table 10. Influence of the percentage of pre- damage on the failure load

Beam name	Middle-span deflections @ Pu (mm)	Ultimate load Pu (kN)	Decrease in the percentage of Pu concerning the reference beam in each group (%)	Decrease in the percentage of Pu concerning the reference solid beam (%)
B-solid-C	102.9	263.7	Ref.	Ref.
B-solid-C-30	90.6	245	7.1	7.1
B-solid-C-60	78.5	204	22.6	22.6
B-solid-C-75	75.5	151	42.7	42.7
B-5Cir-C	90	257	Ref.	2.5
B-5Cir -C-30	70	210	18.2	20.3
B-5Cir -C-60	73	174	32.2	34
B-5Cir-C-75	66	130	49.4	50.7
B-5Squ-C	70	205	Ref.	22.2
B-5Squ-C-30	68	166	19	37
B-5Squ-C-60	70	137.3	33	47.9
B-5Squ-C-75	65	102.4	50	61.2

The percentage of damage is inversely proportional to the ultimate load of the wide beams. These results are consistent with the findings of Yahya Turki & Al-Farttoosi [26]. For the solid beams group, the ultimate load decreased by 7.1, 22.6 and 42.7 for damage percentages of 30, 60 and 75%, respectively, compared to the undamaged strengthened beam. And for the 5 circular opening beam group, the ultimate load decreased by 18.2, 32.2 and 49.4 for damage percentages of 30, 60 and 75%, respectively, compared to the undamaged strengthened beam. Finally, for the 5-square-opening-beam group, the ultimate load decreased by 19, 33, and 50 for damage percentages of 30, 60, and 75%, respectively, compared to the undamaged strengthened beam. Perforated wide beams are more affected by the percentage of damage than solid wide beams.

7.2. Effect of Openings' Shape

Two common shapes of openings (circular and square) were taken here, and thus two sets of wide beams with similar external dimensions and reinforcement were created. The first set consisted of three models perforated with circular holes, the number of which was (3, 5, and 7). The second set consisted of three models perforated with square holes, the area of which was approximately equal to the area of the circular holes, the number of which was (3, 5, and 7). The radius of the circular opening was 60 mm, while the side length of the square opening was 106 mm. Note that the spacing between square openings is the same as that for circular openings, as shown in Figure 14.

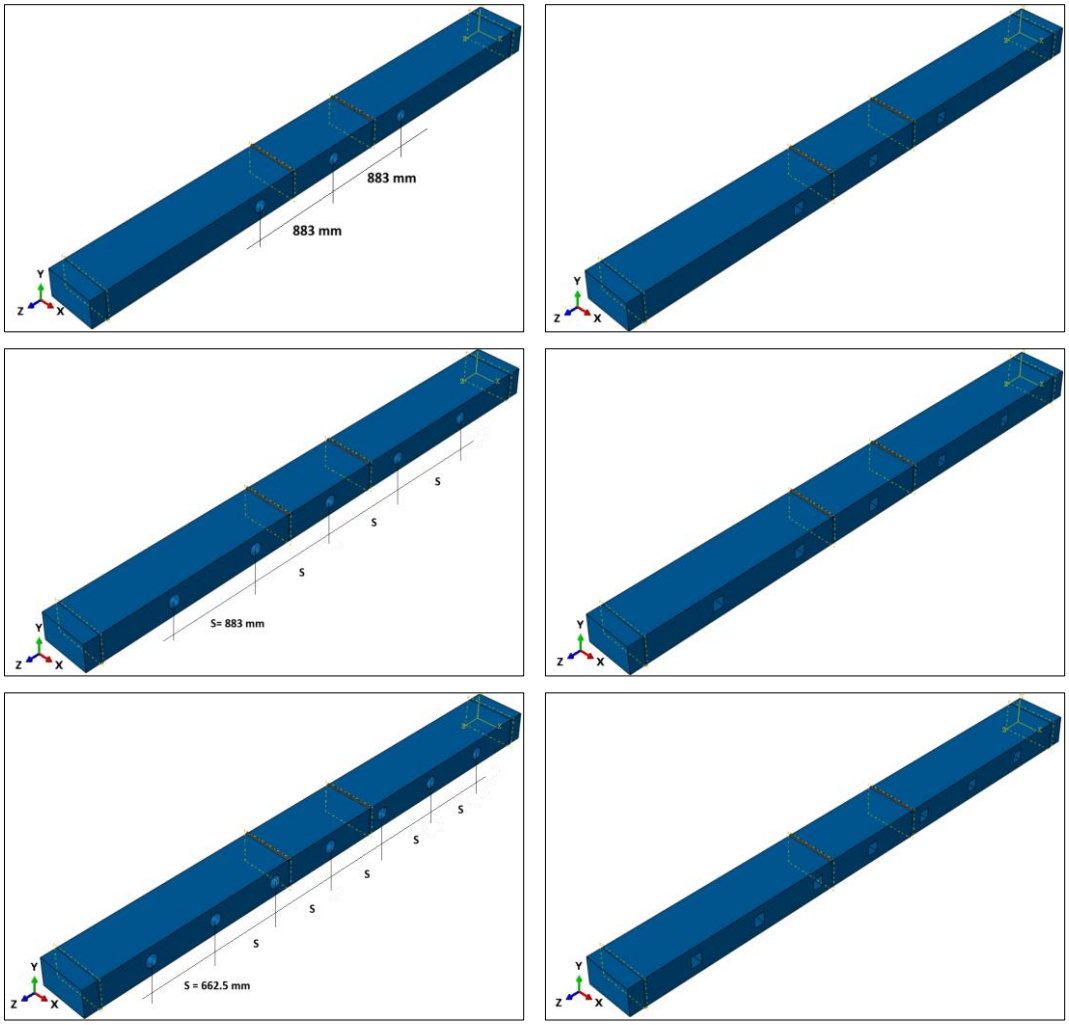

Figure 14. Perforated, undamaged wide beam samples

7.2.1. Load vs. Deflection at Mid-span Relationship

The effect of the openings' shape on the load vs mid-span deflection relation is displayed in Figure 15. Based on load-deflection relationships, it is clear that wide beams with circular openings exhibit higher stiffness than those with square openings, leading to a significant reduction in deflection, especially at service and ultimate stages of loading. The aforementioned findings demonstrate that circular apertures increase the ultimate load-carrying capacity. This is because stresses are concentrated at the corners of square openings, whereas circular openings distribute and reduce them.

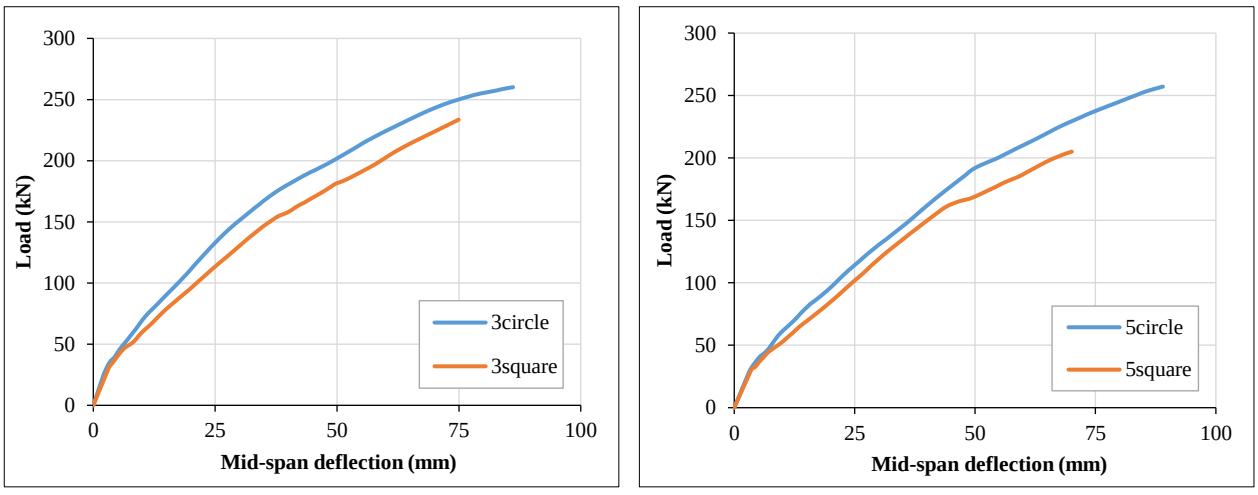

(a) Three openings

(b) Five openings

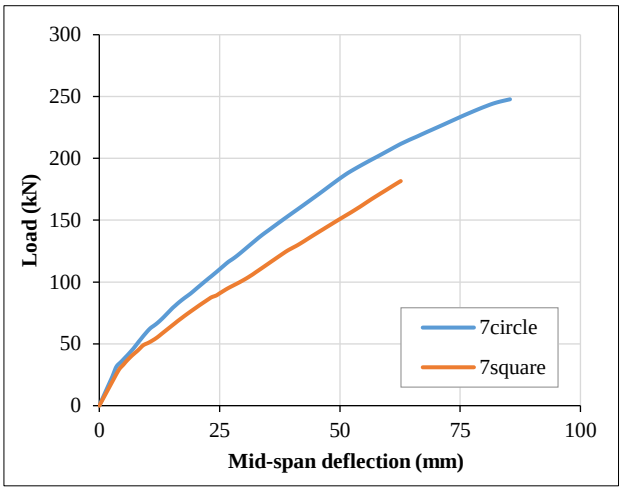

(c) Seven openings

Figure 15. Effect of the openings' shape on the load vs mid-span deflection relationship

7.2.2. Ultimate Load

Figure 16 and Table 11 demonstrate the influence of the openings' shape upon the failure load. The wide beams with circular openings have a higher load-carrying capacity than those with square openings. Using circular holes instead of square ones increases strength by about 11.3%, 25.4%, and 36.5% for three, five, and seven openings, respectively. Circular apertures improve ultimate load-bearing capacity because their circular shape reduces the likelihood of stress concentration around the opening, unlike quadrilateral openings, where stress concentration occurs at angles. It is also noticeable that the advantage of circular openings increases with the number of openings. These results are consistent with the findings of Abdulkareem & Izzet [27] (see Figure 17).

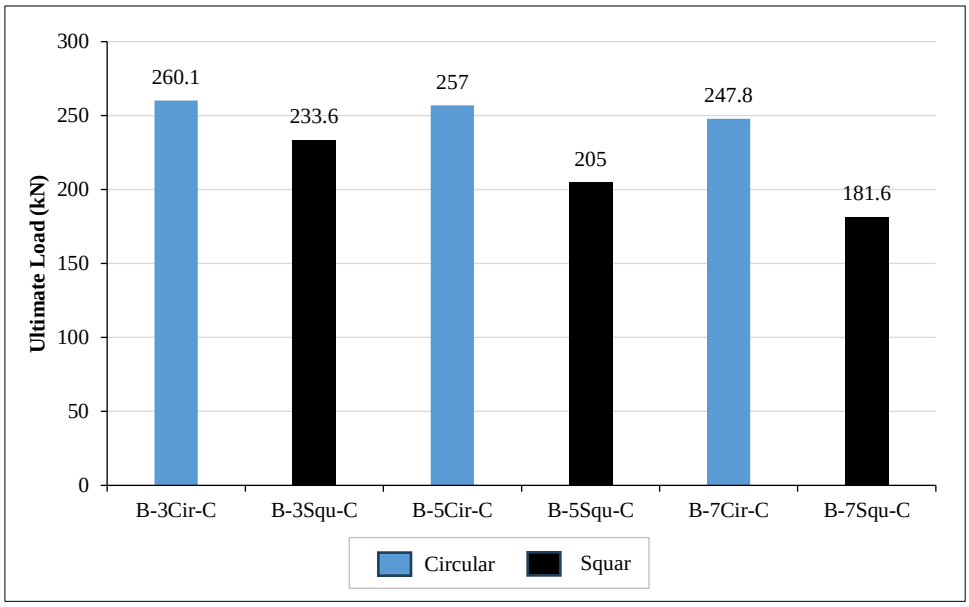

Figure 16. Impact of the openings' shape on the failure load

Table 11. Influence of the openings' shape on the failure load

Beam name	Deflection at Mid-span @ Pu (mm)	Ultimate load Pu (kN)	Increase in the percentage of Pu concerning the circular openings beam in each group (%)
B-3Cir-C	86.1	260.1	Ref.
B-3Squ-C	75	233.6	11.3
B-5Cir-C	90	257	Ref.
B-5Squ-C	70	205	25.4
B-7Cir-C	85.3	247.8	Ref.
B-7Squ-C	62	181.6	36.5

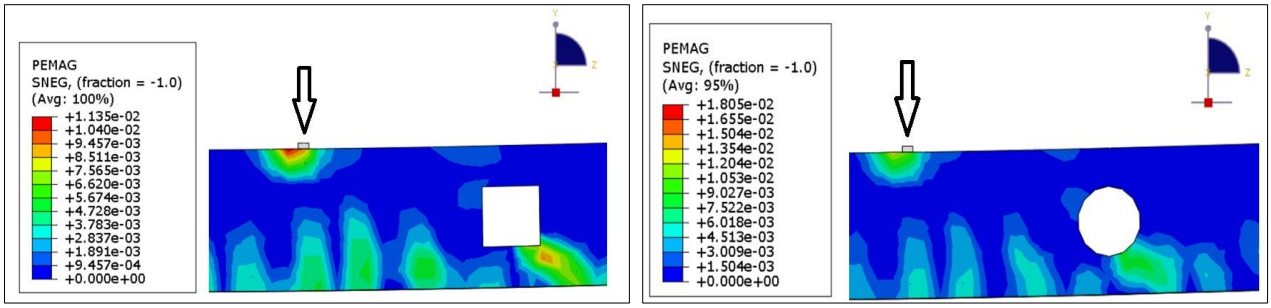

(a) Wide beam with square openings (b) Wide beam with circular openings

Figure 17. Difference between circle and square openings

7.3. Effect of the Number of Openings

Three numbers of openings (3, 5 and 7) were used here, and thus two groups of wide beams with similar external dimensions, numbers of openings and reinforcement were created. The first set consisted of three models perforated with circular holes, the number of which was (3, 5, and 7). The second set consisted of three models perforated with square holes, the area of which was approximately equal to the area of the circular holes, the number of which was 3, 5, and 7 (see Figure 13).

7.3.1. Load-Mid-Span Deflection Relation

The effect of the number of openings on the load vs mid-span deflection relation is depicted in Figure 18. Based on load vs. deflection relationships, it is clear that increasing the number of openings in the wide beams decreases their stiffness, especially at service and ultimate loads.

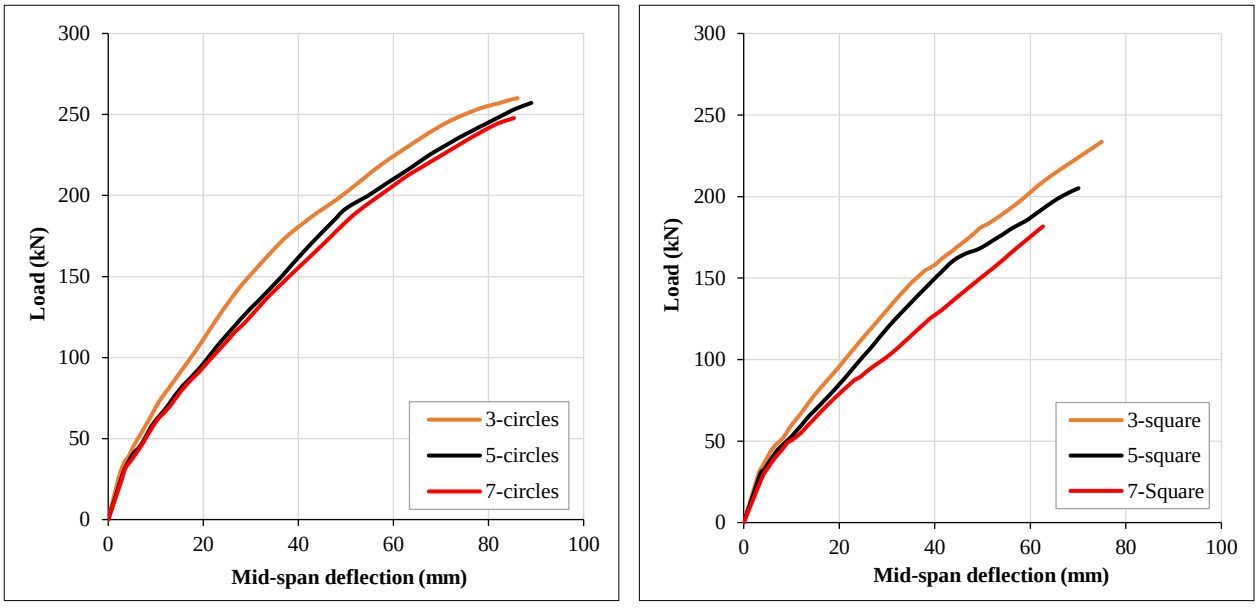

(a) Circle openings (b) Square openings

Figure 18. Effect of the number of openings on the load vs deflection at mid-span relation

7.3.2. Ultimate Load

Table 12 shows that despite openings that weakened the wide beams, strengthening with CFRP laminates restored their load-bearing capacity and even exceeded it. The increase in load-bearing capacity of the strengthened perforated wide beams ranged from 82% to 161% compared to the un- strengthened solid wide beam. The increase in load-bearing capacity of the strengthened solid wide beam was 165% compared to the un- strengthened solid wide beam. In light of this, we conclude that if openings are needed in the wide beam, there is no need to increase their dimensions; rather, the same dimensions can be maintained and reinforced using CFRP. Increasing the number of openings in wide beams reduces their load-bearing capacity. These results are consistent with the findings of Abdulkareem & Izzet [27].

Table 12. Impact of the number of openings on the failure load

Beam ID	CFRP laminate	Ultimate load Pu (kN)	Increase in the percentage of Pu concerning the solid unstrengthened beam (%)	Decrease in the percentage of Pu concerning the solid strengthened beam (%)
B-solid*	without	99.6	Ref.	62.2
B-solid-C**	with	263.7	165	Ref.
B-3Cir-C	with	260.1	161	1.4
B-5Cir-C	with	257	158	2.5
B-7Cir-C	with	247.8	149	6
B-3Squ-C	with	233.6	135	11.4
B-5Squ-C	with	205	106	22.3
B-7Squ-C	with	181.6	82	31.1

* Solid wide beam without CFRP, **Solid wide beam with CFRP.

7.4. Absorbed Energy of All Wide Beams

The absorbed energy of a wide beam is the total energy a structural beam absorbs during deformation, often plastic deformation, under load. Table 13 presents detailed energy measurements for the analyzed wide beams. The perforated wide beams with seven square apertures exhibited the lowest absorbed energy values for the non-damaged beams, attributable to their minimal ultimate load and deflection at ultimate load. In the comparison of analogous broad beams in geometry, the absorbed energy is inversely related to the percentage of damage. By comparing comparable perforated wide beams in terms of the number of holes, the absorbed energy of beams with circular holes is higher than that of beams with square holes. Finally, the absorbed energy is inversely proportional to the number of holes.

Table 13. Absorbed energy of all wide beams

Beam ID	Deflection at Middle-span @ Pu (mm)	Ultimate load Pu (kN)	Absorbed Energy (kN.mm)
B-solid-C	102.9	263.7	16935
B-solid-C-30	90.6	245	13325
B-solid-C-60	78.5	204	9614
B-solid-C-75	75.5	151	6839
B-3Cir-C	86.1	260.1	14764
B-5Cir-C	90	257	14447
B-7Cir-C	85.3	247.8	13087
B-5Cir -C-30	70	210	8053
B-5Cir -C-60	73	174	6958
B-5Cir-C-75	66	130	4700
B-3Squ-C	75	233.6	10620
B-5Squ-C	70	205	8764
B-7Squ-C	62	181.6	6494
B-5Squ-C-30	68	166	6184
B-5Squ-C-60	70	137.3	5265
B-5Squ-C-75	65	102.4	3646

7.5. Stiffness of Beams at the Service Stage for All Wide Beams

Table 14 presents the stiffness during the service level for all wide beams. The selected serviceability threshold was the failure load divided by 1.70, as advocated by several studies, including Mansur et al. [28]. The solid wide beams had the highest initial stiffness. When comparing similar wide beams in the geometry, the stiffness is inversely proportional to the percentage of damage. By comparing comparable perforated wide beams in terms of the number of holes, the stiffness of beams with circular holes is higher than that of beams with square holes. Finally, the stiffness is inversely proportional to the number of holes.

Table 14. Stiffness of all wide beams at the service level

Beam name	Failure-Load Pu (kN)	Service-Load (Ps=Pu /1.7) (kN)	Service-Deflection (D-s) (mm)	Stiffness Ks=Ps/D-s (kN/mm)
B-solid-C	263.7	155.11	41.6	3.729
B-solid-C-30	245	144.11	41	3.515
B-solid-C-60	204	120	35.5	3.380
B-solid-C-75	151	88.82	34.1	2.604
B-3Cir-C	260.1	153	30.7	4.98
B-5Cir-C	257	151.1	41	3.687
B-7Cir-C	247.8	145.7	40.1	3.635
B-5Cir -C-30	210	123.52	36.1	3.421
B-5Cir -C-60	174	102.35	36	2.843
B-5Cir-C-75	130	76.47	33.7	2.2691
B-3Squ-C	233.6	137.4	32.1	4.281
B-5Squ-C	205	120.58	33.3	3.621
B-7Squ-C	181.6	106.8	32	3.338
B-5Squ-C-30	166	97.64	34	2.871
B-5Squ-C-60	137.3	80.76	35.5	2.275
B-5Squ-C-75	102.4	60.23	32.7	1.842

7.6. Ductility Index

The ductility index measures a structural component's ability to withstand large deformations. The proportion of midspan deflections at failure loads to midspan deflections at the tensile main bars' first yielding. By measuring the deflection at the lower steel bars' yield strain at mid-span, the yield deflection was determined. Table 15 shows that the presence of openings in the wide beam reduces the ductility index. Also, the effect of the damage ratio or the shape of the opening on the ductility index is very small.

Table 15. Ductility index of all wide beams

Beam ID	Ultimate deflection at the middle span D-u (mm)	Yield-Deflection at middle-span (D-y) (mm)	Ductility index = D-u / D-s
B-solid-C	102.9	52.5	1.96
B-solid-C-30	90.6	52.5	1.73
B-solid-C-60	78.5	46	1.71
B-solid-C-75	75.5	45	1.68
B-3Cir-C	86.1	45	1.91
B-5Cir-C	90	54	1.67
B-7Cir-C	85.3	53.5	1.59
B-5Cir -C-30	70	45.5	1.54
B-5Cir -C-60	73	48	1.52
B-5Cir-C-75	66	44	1.5
B-3Squ-C	75	41.9	1.79
B-5Squ-C	70	43.5	1.61
B-7Squ-C	62	40	1.55
B-5Squ-C-30	68	44.2	1.538
B-5Squ-C-60	70	46.2	1.52
B-5Squ-C-75	65	43	1.51

7.7. Crack Patterns at the Ultimate Load Stage

According to the CDP theory, cracks in reinforced concrete members typically occur in areas where tensile strain exceeds the specified tensile strain of concrete. In other words, concrete will crack when the plastic strain exceeds zero.

Therefore, in this study, the maximum plastic principal strain was used as an indicator of crack development. It is hypothesized that the fractures are orthogonal to the maximal primary plastic strain (PEMAG). Therefore, it is possible to gain a good understanding of the failure pattern from the Abaqus program. Figures 19 to 25 show the cracking pattern for some wide beams, and from them, we can deduce the following:

- All solid wide beams, whether reinforced with CFRP or not, failed due to yielding of the steel reinforcement, followed by compression failure. Nevertheless, the undamaged, unreinforced beam had broader fissures concentrated in the middle region. The use of CFRP laminates on the beam's bottom surface reduces fracture breadth and disperses it over a wider area.
- The damage percentage level did not change the pattern of failure.
- The perforated wide beams (strengthened with CFRP or not) failed by diagonal splitting near the nearest opening to the load point, followed by compression failure.

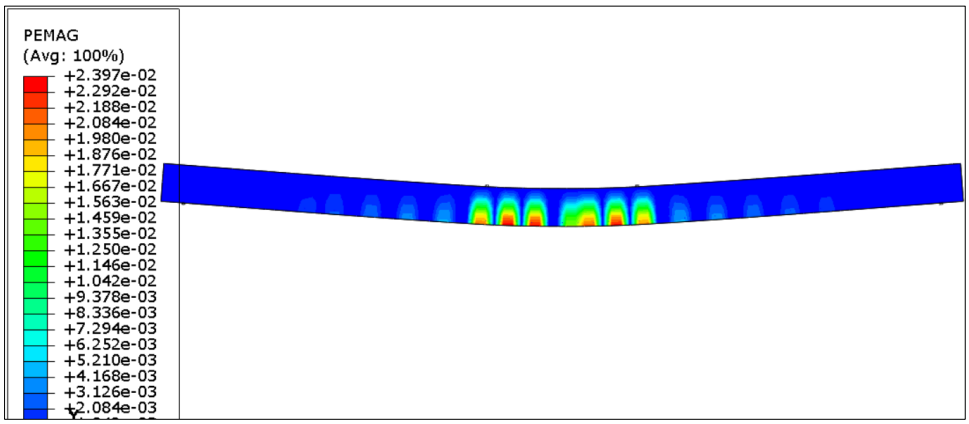

Figure 19. Crack shape of B-solid

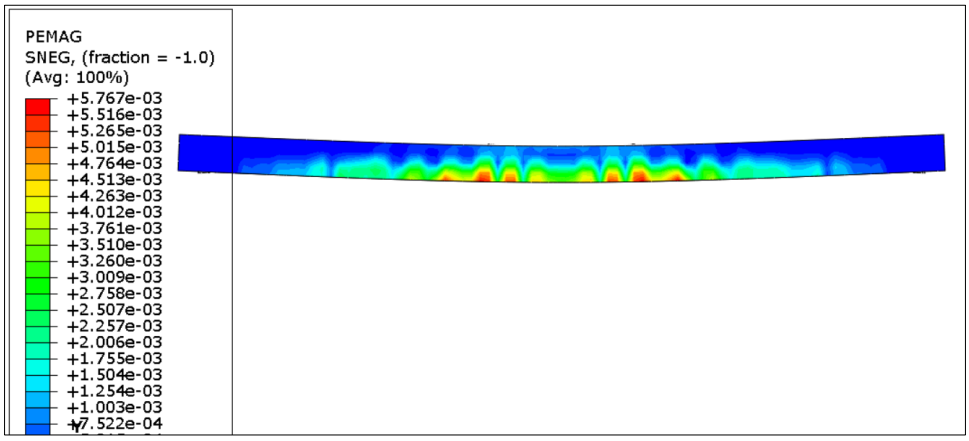

Figure 20. Crack shape of B-solid-c-30

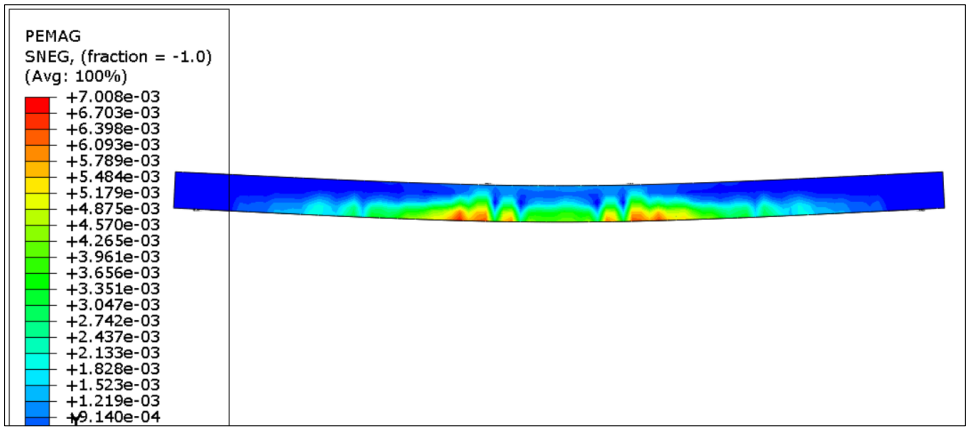

Figure 21. Crack shape of B-solid-c-75

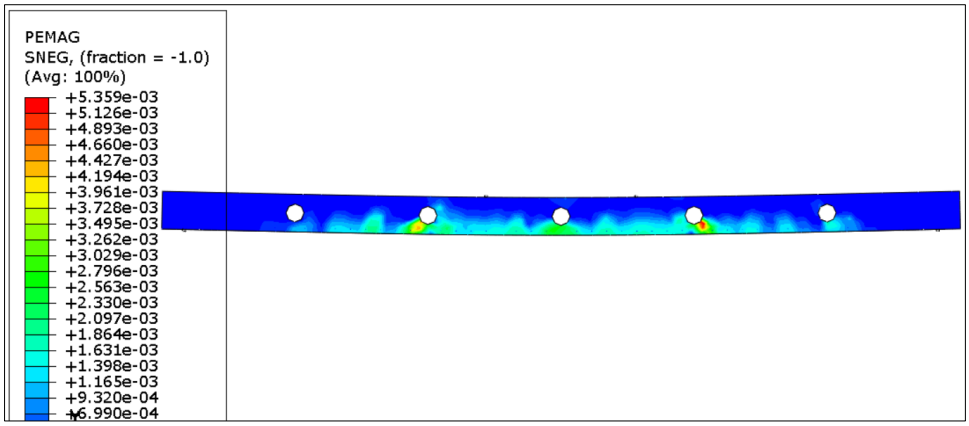

Figure 22. Crack shape of B-5Cir-C-30

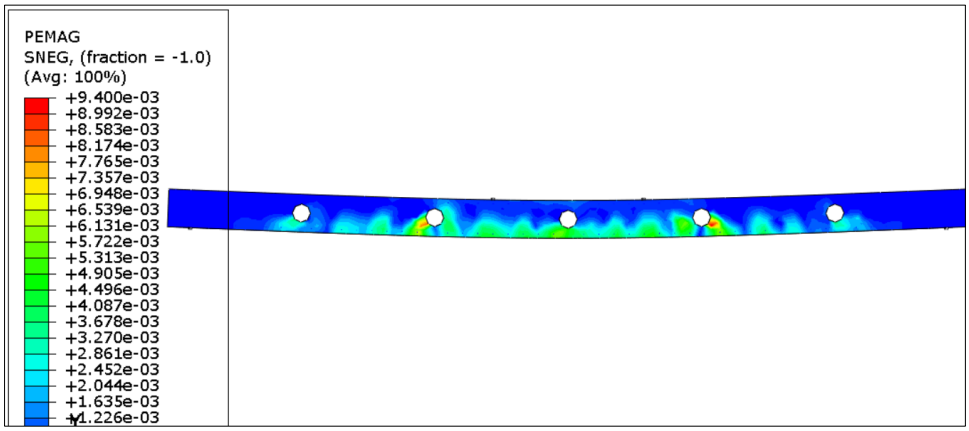

Figure 23. Crack shape of B-5Cir-C-60

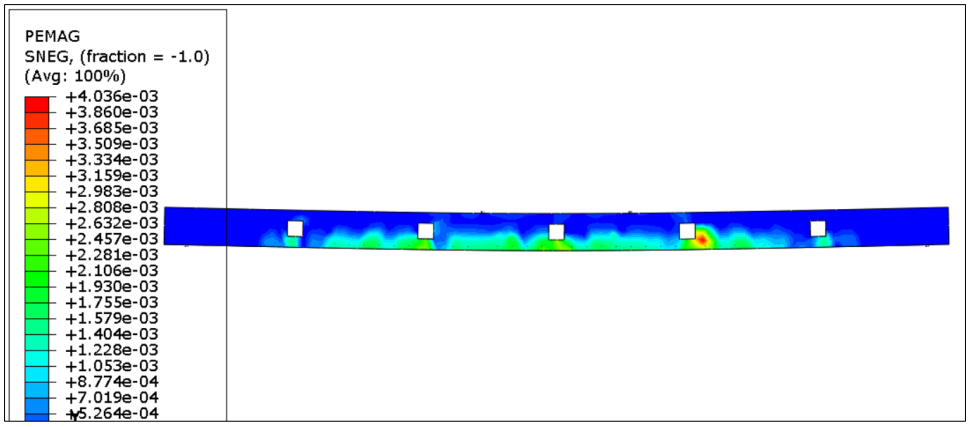

Figure 24. Crack shape of B-5Squ-C-30

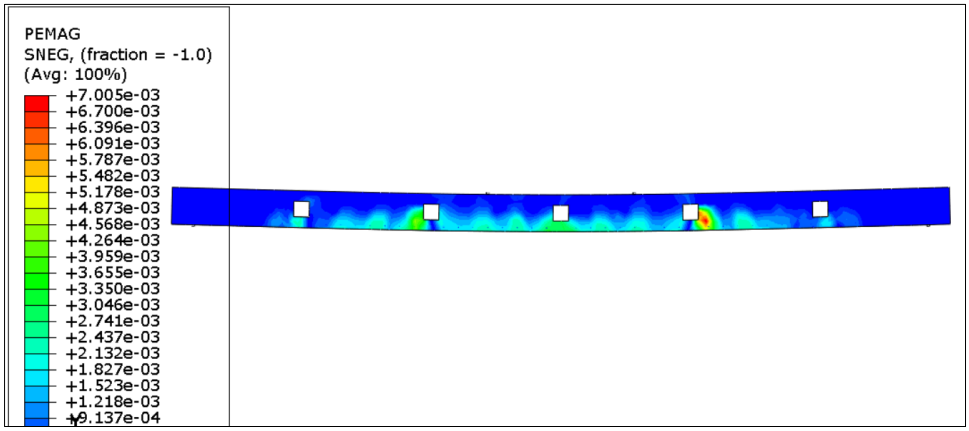

Figure 25. Crack shape of B-5Squ-C-60

8. Conclusions

The main conclusions drawn from this study are summarized as follows:

- A strong correlation was observed between the ultimate load and mid-span deflection values obtained from finite element models and from experiments, with the mean and coefficient of variation of (Pu) FE/(Pu) Ex being 1.025 and 2.0158%, respectively, for failure loads. In contrast, for deflection at mid-span (Δu FE / Δu Ex), they were 0.9735 and 4.269%, respectively.
- The damage percentage is inversely related to the ultimate load of the broad beams. In the solid beams group, the ultimate load decreased by 7.1, 22.6, and 42.7 for damage percentages of 30%, 60%, and 75%, respectively, when compared to the undamaged reinforced beam. For the group of five circular opening beams, the ultimate load decreased by 18.2, 32.2, and 49.4 for damage percentages of 30%, 60%, and 75%, respectively, compared with the undamaged reinforced beam. For the set of beams with five square openings, the ultimate load decreased by 19, 33, and 50 for damage percentages of 30%, 60%, and 75%, respectively, when compared to the undamaged reinforced beam. Perforated broad beams are evidently more influenced by the extent of damage compared to solid wide beams.
- Wide beams with circular holes have a higher load-bearing capacity than those with square apertures. Using circular apertures instead of square ones yields strength improvements of 11.3%, 25.4%, and 36.5% for three, five, and seven openings, respectively. The circular apertures improve the ultimate load-bearing capacity owing to their design, which reduces potential stress concentration around the opening, unlike square openings, where stress concentration increases at the corners. The advantage of circular apertures becomes more evident as the number of openings increases.
- Notwithstanding apertures that compromised the integrity of the wide beams, reinforcement with CFRP laminates reinstated their load-bearing capacity and exceeded it. The enhanced load-bearing capacity of the fortified perforated wide beams ranged from 82% to 161% compared to the unreinforced solid wide beam. The enhanced load-bearing capability of the fortified solid wide beam was 165% more than that of the unfortified solid wide beam. Consequently, we determine that if apertures are required in the broad beam, it is unnecessary to augment their diameters; instead, the existing dimensions may be preserved and strengthened using CFRP.
- Increasing the number of openings in the wide beams reduces their load-bearing capacity.
- By comparing comparable wide beams in the geometry, the absorbed energy is inversely proportional to the percentage of damage. By comparing comparable perforated wide beams in terms of the number of holes, the absorbed energy of beams with circular holes is higher than that of beams with square holes. Finally, the absorbed energy is inversely proportional to the number of holes.
- When comparing similar wide beams in the geometry, the stiffness is inversely proportional to the percentage of damage. By comparing comparable perforated wide beams in terms of the number of holes, the stiffness of beams with circular holes is higher than that of beams with square holes. Finally, the stiffness is inversely proportional to the number of holes.
- All solid broad beams, whether reinforced with CFRP or not, failed due to yielding of the steel reinforcement, followed by compression failure. Nonetheless, in the intact, unfortified beam, the fissures were broader and centered in the core region. The use of CFRP laminates on the beam's bottom surface reduces fracture breadth and disperses it over a wider area. The perforated broad beams, whether reinforced with CFRP or not, exhibited diagonal splitting failure near the opening closest to the load point, followed by compression failure.
- The presence of openings in the wide beam reduces the ductility index's value. Also, the effect of the damage ratio or the shape of the opening on the ductility index is very small.

9. Declarations

9.1. Author Contributions

Conceptualization, B.F.A., T.H.I., H.K.M., and A.A.A.; methodology, B.F.A., T.H.I., H.K.M., and A.A.A.; software, investigation, B.F.A., T.H.I., H.K.M., and A.A.A.; writing—original draft preparation, B.F.A., T.H.I., H.K.M., and A.A.A.; writing—review and editing, B.F.A., T.H.I., H.K.M., and A.A.A. All authors have read and agreed to the published version of the manuscript.

9.2. Data Availability Statement

The data presented in this study are available upon request from the corresponding author.

9.3. Funding

The authors received no financial support for the research, authorship and/or publication of this article.

9.4. Conflicts of Interest

The authors declare no conflict of interest.

10. References

[1] Conforti, A., Minelli, F., & Plizzari, G. A. (2013). Wide-shallow beams with and without steel fibres: A peculiar behaviour in shear and flexure. Composites Part B: Engineering, 51(1), 282–290. doi:10.1016/j.compositesb.2013.03.033.

[2] Soliman, A. A., Mansour, D. M., Ebid, A., & Khalil, A. H. (2023). Shallow and Wide RC Beams, Definition, Capacity and Structural Behavior – Gap Study. The Open Civil Engineering Journal, 17(1). doi:10.2174/18741495-v17-e230725-2023-28.

[3] Mahmoud, S. M., Mabrouk, R. T. S., & Kassem, M. E. (2021). Behavior of RC wide beams under eccentric loading. Civil Engineering Journal (Iran), 7(11), 1880–1897. doi:10.28991/cej-2021-03091766.

[4] Abdulkareem, B., & Izzet, A. F. (2022). Serviceability of Post-fire RC Rafters with Openings of Different Sizes and Shapes. Journal of Engineering, 28(1), 19–32. doi:10.31026/j.eng.2022.01.02.

[5] Abdulkareem, B. F., & Izzet, A. F. (2021). Post Fire Residual Concrete and Steel Reinforcement Properties. IOP Conference Series: Earth and Environmental Science, 856(1), 12058. doi:10.1088/1755-1315/856/1/012058.

[6] Alobaidi, H. E., & Al-Zuhairi, A. H. (2023). Structural Strengthening of Insufficiently Designed Reinforced Concrete T-Beams using CFRP Composites. Civil Engineering Journal, 9(8), 1880–1896. doi:10.28991/CEJ-2023-09-08-05.

[7] Abdulkareem, B. F., Ibrahim, T. H., Mohammed, H. K., & Allawi, A. A. (2025). Study on Shear Behavior of Reinforced Concrete Beams Confined with Reinforcing Meshes. Civil Engineering Journal, 11(10), 4211–4231. doi:10.28991/CEJ-2025-011-10-012.

[8] Tahera, & Urs, N. (2025). Performance evaluation and deep learning-based prediction of CFRP-strengthened RC beams with core-cut openings. Asian Journal of Civil Engineering, 27(1), 59–87. doi:10.1007/s42107-025-01490-w.

[9] Alasmari, H. A., Sharaky, I. A., Elamary, A. S., & El-Zohairy, A. (2025). Rehabilitation and Strengthening of Damaged Reinforced Concrete Beams Using Carbon Fiber-Reinforced Polymer Laminates and High-Strength Concrete Integrating Recycled Tire Steel Fiber. Fibers, 13(1), 10. doi:10.3390/fib13010010.

[10] Lotfy, E. M., Mohamadien, H. A., & Hassan, H. M. (2014). Effect of web reinforcement on shear strength of shallow wide beams. International Journal of Engineering and Technical Research (IJETR), 2(11), 98-107.

[11] Conforti, A., Minelli, F., Tinini, A., & Plizzari, G. A. (2015). Influence of polypropylene fibre reinforcement and width-to-effective depth ratio in wide-shallow beams. Engineering Structures, 88(1), 12–21. doi:10.1016/j.engstruct.2015.01.037.

[12] El-Sayed, A. K., Al-Zaid, R. A., Al-Negheimish, A. I., Shuraim, A. B., & Alhozaimy, A. M. (2014). Long-term behavior of wide shallow RC beams strengthened with externally bonded CFRP plates. Construction and Building Materials, 51(1), 473–483. doi:10.1016/j.conbuildmat.2013.10.055.

[13] Chin, S. C., Shafiq, N., & Nuruddin, M. F. (2016). Behaviour of RC beams with CFRP-strengthened openings. Structural Concrete, 17(1), 32–43. doi:10.1002/suco.201400111.

[14] Abass, A. L., & Hassan, Y. R. (2017). Flexural Strengthening of Reinforced Concrete Wide Beams with Different Width of CFRP. Diyala Journal of Engineering Sciences, 10(3), 14–29. doi:10.24237/djes.2017.10302.

[15] Al-Abdwais, A. H., & Al-Mahaidi, R. S. (2021). Experimental and finite element analysis of flexural performance of RC beams retrofitted using near-surface mounted with CFRP composites and cement adhesive. Engineering Structures, 241, 112429. doi:10.1016/j.engstruct.2021.112429.

[16] Al-Kamaki, Y. S. S. (2025). Flexural Repair of Pre-Loaded and Pre-Damaged RC Beams Using Anchored Hybrid FRP Composites. Civil and Environmental Engineering, 21(2), 1113–1126. doi:10.2478/cee-2025-0083.

[17] Badawy, M. M., Anan, A. I., Elkadi, O. A., & Sayed-Ahmed, E. Y. (2024). Flexural behavior of high strength concrete shallow wide beams reinforced by hybrid longitudinal reinforcement. HBRC Journal, 20(1), 205-230. doi:10.1080/16874048.2024.2309818.

[18] Palaniappan, K., Joanna, P. S., Rajasekaran, M., Prabhavathy, A., Cruze, D., & James, S. (2025). Flexural behaviour of pre-damaged RC beams retrofitted using CFRP laminates. Advances in Civil and Architectural Engineering, 16(30), 55–66. doi:10.13167/2025.30.4.

[19] Askar, M. K. (2025). Rehabilitation of Pre-Damaged RC Beam Containing Recycled Plastic Waste Using CFRP. Al-Rafidain Engineering Journal, 30(1), 164–174. doi:10.33899/arej.2024.152874.1370.

[20] Al-Negheimish, A. I., El-Sayed, A. K., Al-Zaid, R. A., Shuraim, A. B., & Alhozaimy, A. M. (2012). Behavior of Wide Shallow RC Beams Strengthened with CFRP Reinforcement. Journal of Composites for Construction, 16(4), 418–429. doi:10.1061/(asce)cc.1943-5614.0000274.

[21] Al-Zaid, R. A., El-Sayed, A. K., Al-Negheimish, A. I., Shuraim, A. B., & Alhozaimy, A. M. (2014). Strengthening of structurally damaged wide shallow RC beams using externally bonded CFRP plates. Latin American Journal of Solids and Structures, 11(6), 946–965. doi:10.1590/S1679-78252014000600003.

[22] Dassault Systèmes. (2022). User's Manual, Ver. 2019. Dassault Systèmes, Johnston, United States.

[23] Majumder, S., & Saha, S. (2021). Shear behaviour of RC beams strengthened using geosynthetic materials by external and internal confinement. Structures, 32, 1665–1678. doi:10.1016/j.istruc.2021.03.107.

[24] Dassault Systemes Simulia Corp. (2012) Abaqus Analysis User's Manual (Version 6.12). Dassault Systemes, Providence, Fremont, United States.

[25] Kachlakev, D. I., Miller, T. H., Potisuk, T., Yim, S. C., & Chansawat, K. (2001). Finite element modeling of reinforced concrete structures strengthened with FRP laminates. FHWA-OR-RD-01-XX, U.S. Department of Transportation, Washington, United States.

[26] Yahya Turki, A., & Al-Farttoosi, M. H. (2023). Investigation of the Stiffness and Ductility of Pre-Cracked RC Beams after repairing with CFRP using Different Strengthening Methods. Engineering, Technology and Applied Science Research, 13(6), 12423–12426. doi:10.48084/etasr.6555.

[27] Abdulkareem, B. F., & Izzet, A. F. (2022). Residual post fire strength of non-prismatic perforated beams. IOP Conference Series: Earth and Environmental Science, 961(1), 12002. doi:10.1088/1755-1315/961/1/012002.

[28] Mansur, M. A., Huang, L. M., Tan, K. H., & Lee, S. L. (1992). Deflections of reinforced concrete beams with web openings. ACI Structural Journal, 89(4), 391–397. doi:10.14359/3019.